MAJOR ROLE OF COMPUTATIONAL FLUID DYNAMICS, SPECIFICALLY THE PREDICTION OF AERODYNAMIC PROPERTIES, IN THE DESIGN PROCESS OF THE AUTOMOBILE INDUSTRY

[1]N.Yuganand, [2]G.Naresh Reddy, [3]K.Venkanna, [4]Kamera Tirupati

[1,2,3]Assistant Professor, [4]UG Student, [1,2,3,4]Department of H&S, Brilliant Grammar School Educational Society Group of Institutions Integrated Campus, Hyderabad, India

Abstract

Aerodynamics makes for more than 70% of the Formula 1 variables that may be affected by engineers. In the design process for the automobile industry, computational fluid dynamics is becoming more and more important, particularly for the forecasting of aerodynamic properties. The modelling of the aerodynamic flow around a Formula 1 racing car's front end is the focus of the current study. There were four stages to the numerical simulation: modelling of the geometry, creation of the computational mesh, computing of the flow, and visualisation and analysis of the flow solutions. The flow computation was carried out on a high-performance parallel computer system, the Silicon Graphics Origin2000, due to the substantial resources required. Comparison of the numerical predictions with wind tunnel data shows that the correct dependencies of the aerodynamic forces on various tuning parameters are obtained. Thus, despite the complexity of both the car geometry and the flow behaviour, the present study has shown that numerical simulation can provide a wealth of information useful to the design process

Introduction

An essential factor in a Formula 1 racing car's performance is aerodynamics. It is possible to specify a variety of essential flow zones, including the front and rear wings, the air intakes, the underbody, and the diffuser. These regions have extraordinarily complicated, turbulent, and three-dimensional flow. Moreover, the flow in various locations is linked; in fact, the performance of the vehicle is determined by its total aerodynamic behavior.

A Formula 1 racing car's aerodynamic forces may be altered by adjusting several aspects of the vehicle and its add-ons. The main objective is to provide the most down force possible to improve stability, especially while cornering, and power transmission from the engine. In order to optimize the performance of the car, it is important to determine how the aerodynamic forces vary with the tuning of various parameters such as road height, wing configuration and flap angles.

Numerical flow simulation has not been extensively employed initially for Formula 1 aerodynamic design for essentially two reasons:

due to the complexity of the flow, large-scale numerical simulations require advanced numerical software and substantial computational resources that have not been available,

as in other application areas, there is reluctance to embrace a new technique such as Computational Fluid Dynamics (CFD) until it has been proven to provide useful and reliable information.

Aided by the continual development of computer software and hardware, a number of Formula 1 teams have begun using CFD for aerodynamic design. While numerical simulation can not entirely replace existing experimental methods, it has a number of potential uses and advantages:

a. to reduce the dependence on - and cost of – wind tunnel testing
b. since it provides local values of the flow quantities (e.g. pressure, velocity) throughout the flow domain, significantly more information is available
c. certain aspects can be simulated more easily numerically than experimentally (e.g. cornering with front wheels having a non-zero yaw angle)
d. with increasing computer software and hardware capabilities, the turnaround time for numerical simulations can be shorter than for windtunnel testing.

Geometries and Flow Conditions

A number of different front-end configurations have been considered in this study. These configurations have been defined at Sauber Petronas Engineering AG. The present seminar will concentrate on one particular configuration, which is shown in Fig. 8. This configuration consists of a front wing assembly, a nose section and two connecting pylons, and a ground plane. In addition, the two front wheels are included to

account for flow blockage effects. To avoid large flow perturbation associated with an abrupt trailing edge, a reversed section is attached at the back of the nose section. The wing assembly consists of a main plane and, for this configuration, one flap. The wing is terminated laterally in side plates that have recessed sections near the trailing edge. The configuration is symmetric with respect to the central vertical plane (y=0).

To investigate the influence of ground effects, two different ride heights were considered. In addition, to study the flow blockage effect of the wheels, the influence of moving the wheels inboard and eliminating them completely was also investigated.

Two different free stream conditions were considered, 35 m/s and 70 m/s. For all computations the flow was considered to be fully turbulent. No-slip boundary conditions were applied to the wing and nose sections, i.e. the velocity on these surfaces was set to zero. The velocity of the ground plane was set to the free stream velocity. On the surface of the wheels, the tangential velocity was set to the free stream velocity, to simulate the rotation of the wheels.

Numerical Tools:

Software

Numerical flow simulation consists of resolving the governing flow equations- the Navier-Stokes equations - throughout the flow domain. Numerical simulation is comprised of four main phases:

a. geometry modeling
b. mesh generation
c. flow computation
d. solution analysis.

For the present application, the flow is subsonic and can be considered to be incompressible. The geometry considered is sufficiently complex to profit from the increased flexibility of completely unstructured mesh techniques.With these considerations, the following softwares were employed for the numerical simulation:

a. DDN (ICEM) CAD system for geometry importing and modification
b. PCube (ICEM) for (triangular) surface mesh generation
c. TGrid (Fluent) for (tetrahedral) volume mesh generation
d. Fluent/UNS for flow computation
e. Fluent/UNS for post-processing

All of the above software are incorporated into the commercial Fluent package, facilitating transfer of data between the different simulation phases. This software package represents the state of the art in numerical simulation, is widely used for industrial applications (including by other Formula 1 racing teams), and has been adopted by the Fluid Mechanics Laboratory (LMF) as its main commercial flow software.

Hardware

The geometry modeling and mesh generation phases could be performed on workstations (DDN, PCube and TGrid are installed on Silicon Graphics and Hewlett Packard workstations at the LMF), the flow computation and subsequent solution analysis were performed on a high-performance parallel computer system, a 32-processor Silicon Graphics Origin2000 installed at the EPFL. Due to availability limitations, only 6 processors of the Origin2000 were used for the flow computations in the present study, although use of a greater number of processors would have shortened turn-around time. It should be noted that while the flow computation phase required the major proportion of computer time, the mesh generation phase was substantially more engineer-time intensive.

Computational Aspects:

Geometry Modelling:

The configurations employed in this study have been designed using the CATIA CAD system at Sauber Petronas Engineering AG, and correspond to models that have been tested in the windtunnel at SF-Emmen. The geometrical description of the configurations was supplied to the LMF in standard IGES format. Only slight modifications of these descriptions were found necessary for use in the numerical simulation procedure.

Mesh Generation

Due to the strong interaction between the quality of the computational mesh and the accuracy of the resulting flow solution, a substantial effort was made in the mesh generation phase.

The generation of suitable computational meshes was performed in two stages: triangulation of all surfaces, followed by the creation of a tetrahedral mesh in the volume bounded by these surfaces. The surface mesh creation is by far the most complex and time-consuming; while surface mesh generation using PCube is

very flexible, it is also very user-intensive. Creation of the 3D volume meshes for the present study was performed with TGrid, which uses a robust, fast and highly automated Delaunay method that requires little time or effort.

To aid in the surface mesh generation, the geometry is divided into separate parts (e.g. wing main plane, flap, side plate, body, wheels, ground plane, etc.) and the individual surfaces meshed separately. These are then assembled to form the complete surface mesh for the computational domain. This has the advantage that, modifications to the geometry (e.g. changes in the wing, ride height and wheel positions) can be accommodated without a major investment of effort.

The computational domain for the present application was chosen to be a box of sufficiently large extent such that the position of the external freestream boundaries has essentially no influence on the computed flow. Surface mesh cells were concentrated in regions considered to be of most importance, e.g. on the wing. Surfaces of lesser interest, e.g. the wheels, have been allocated less mesh cells, leading to a lower accuracy in the flow solution in neighbouring regions. A global view of the resulting surface mesh is shown in Fig.2. After the generation of the volume mesh, a computational mesh with a total of 1,144,000 cells and 260,000 nodes was obtained for this configuration (although over 1.5 million mesh cells have been employed for other configurations).

Flow Computation:

The governing flow equations were resolved using Fluent/UNS. This flow solver uses a cell-centered finite volume discretization on an unstructured mesh, with a SIMPLE algorithm to couple the pressure and velocity fields. To obtain maximum

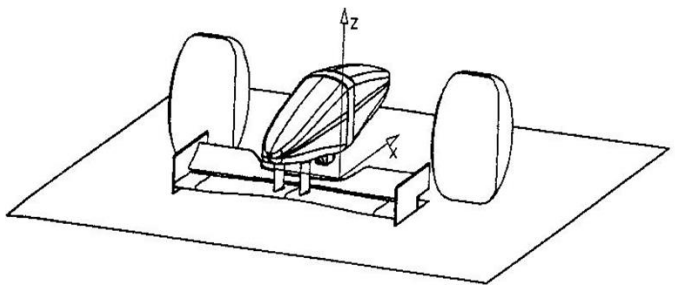

Figure 1. Front end configuration

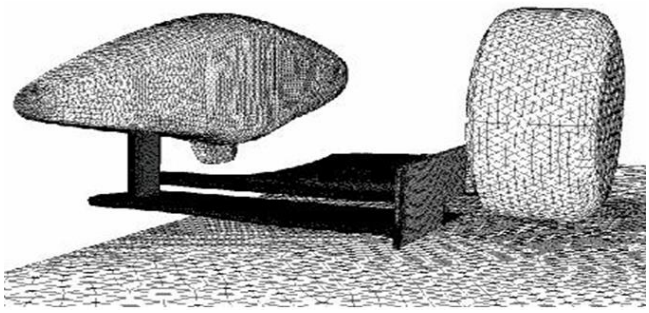

Figure 2. Surface mesh on half of the front-end configuration

(that measure how well each of the flow equations are satisfied) and the lift and drag on the wing surfaces were monitored during the iteration procedure. While convergence of the residual values was not observed, the lift and drag coefficients converged to at least three significant figures. These results indicate that the computed flow solution contains local regions of unsteady flow. A closer examination of the flow solution indicated that these regions were associated with the large separated region behind the wheels. Since the present study does not aim to simulate accurately the flow behind the wheels (indeed there are insufficient mesh cells to do so), the observed convergence behaviour is considered to be acceptable.

Results

Numerical flow simulations produce a wealth of data, which can be represented in a number of different manners. Only a selection of these representations are presented here. They can be divided into two classes: local flow fields that provide specific insights into the behaviour of the flow, and global forces that indicate the overall aerodynamic properties.

Local Flow fields:

A perspective view of the contours of static pressure computed on the surfaces of the front-end section of the Formula 1 racing car is shown in Fig.3

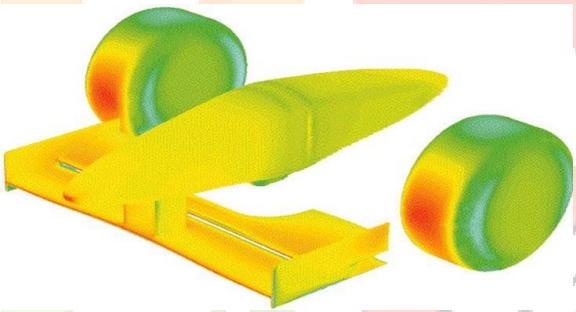

Figure 3: Perspective view of the computed surface pressure on the front-end configuration (red: high pressure; blue: low pressure)

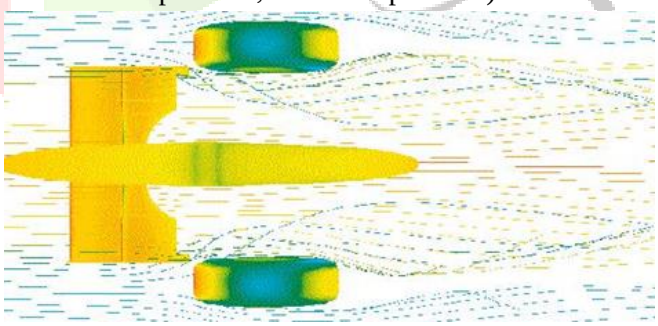

Figure 4. Plan view of the computed streamlines around the front-end configuration

These views show localized regions of high pressure at the leading edges of the nose, wing, pylons and wheels. Pressure depression is computed, as expected, on the lower surface of the wings and side and rear surfaces of the wheels.

For steady flows, streamlines trace the paths taken by fluid elements; they can thus provide insights into the flow behaviour, such as the influence of various geometry parts on the flow and the presence of vortices. Fig. 4. represents the computed streamlines emitted from a rake placed horizontally upstream of the front wing perpendicular to the flow.

Figure 4. also shows that the streamlines pass essentially undeflected laterally around and downstream of the wing, although the wheels provide a major disturbance to the flow. The trailing vortices that are generated at the side plates are not clearly apparent due to the close proximity of the wheels, resulting in a complex large-scale vortex system observed in the flow region downstream of the wing. Directly under the
body, only a slight lateral displacement of the streamlines is observed. Finally, locating the wheels inboard was found not to result in major global modifications of the flow fields, as discerned from the streamline plots. Nevertheless, when the wheels are almost centrally located behind the side plates, they appear to cause an increased damping of the wing trailing vortices.

The aerodynamic forces exerted on the surface of each part of the geometry are available directly from Fluent/UNS. In the present paper, the aerodynamic forces exerted on the wing/body geometry (comprised of the wing elements, side plates, pylons and body) are considered. From the computed forces and corresponding moments, the centre of pressure of the wing/body geometry can be determined; the centre of pressure can be defined as the point in space (not necessarily on the geometry) about which the total aerodynamic moments are zero.

Fig. 5 shows the computed downforce (F_z) and drag (F_x) exerted on the wing/body geometry for two different road heights. Also shown in this figure are the corresponding values determined experimentally from wind tunnel tests. As may

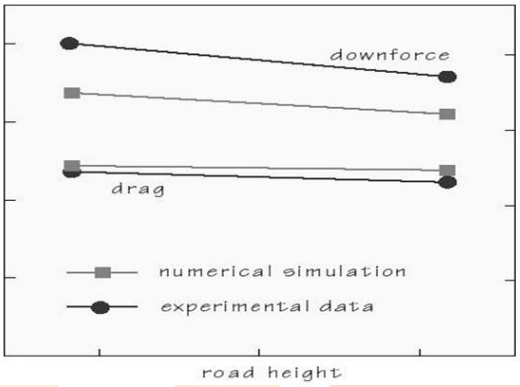

Figure5. Comparison of computed and measured values of the downforce (top) and drag (bottom) exerted on the wing/body geometry as a function of road height

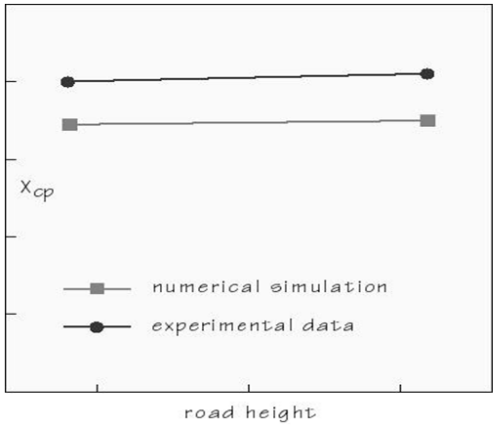

Figure6. Comparison of computed and measured values of the streamwise component of the centre of pressure as a function of road height

be expected, the downforce is greater for the smaller ride height, due to the increased influence of the well-known ground effect. The dependence of the drag on the road height is observed to be significantly smaller. A quantitative difference can be observed between the measured downforce values and those predicted by the numerical simulations.

numerical accuracy, the second-order upwind scheme was applied for the convection terms, with the diffusion terms discretized using a central difference approximation. The discretized equations were resolved using a Gauss-Seidel method coupled with a multigrid acceleration technique. For parallel computation on the Silicon Graphics Origin2000, the computational mesh was partitioned using the coordinate bisection method into sub-meshes, and the resolution of the flow

equations on each sub-mesh computed on a different processor. Both the mesh partitioning and parallel computation was handled by Fluent/UNS in a transparent manner.

For all the computations performed, it was assumed that the flow was steady; thus an iterative procedure is performed until convergence to a steady state solution is hopefully achieved. Both the residuals

The dependence of both the downforce and the drag on road height are correctly predicted. This is important, since it is the dependencies rather than the absolute values that are important for design optimization.

Numerical simulations performed for the configuration considered in this paper show that the lift and drag coefficients (i.e. the downforce and drag normalized to the square of the freestream velocity) exhibit only a slight dependence on the freestream velocity. This observation, which indicates that viscous behavior is similar at the two flow velocities considered, is corroborated by the windtunnel measurements.

Fig. 6 shows the computed and measured values of the streamwise component of the centre of pressure of the wing/body geometry for two different road heights. The centre of pressure is seen to shift slightly backward as the ride height is increased.

Finally, the wheels are observed to have a significant influence on both the lift and drag exerted on the rest of the geometry. The values of the downforce on the wing/body geometry presented in Fig. 14 shows that the downforce decreases when the wheels are moved inboard, due to the increased blockage of the flow induced by the wheels. Fig. 6 also shows that the downforce increases, as expected, if the wheels are completely removed. The dependence of the downforce with the change in wheel position is observed to be well predicted by the numerical simulations. However, the change in the downforce on removal of the wheels is computed to be significantly higher than measured. This latter observation may be associated with the fact that the numerical simulation of the flow around the wheels lacks accuracy due to an insufficient local density of mesh cells.

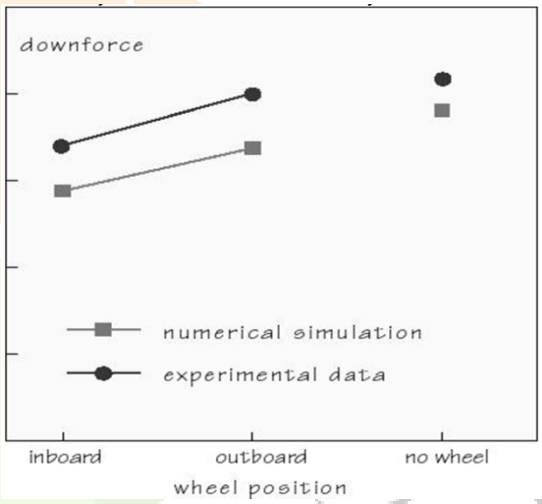

Figure 7. Comparison of computed and measured values of the downforce as a function of wheel position.

Conclusion

CFD is a new “third dimension” in fluid dynamics, equally sharing the stage with the other dimensions of pure theory and pure experiments. i.e. CFD enables the user to get a 3-dimensional virtual reality not only visually but supported by computations which otherwise would be very complex to solve. It has reduced research time to nearly about one-fourth of previous time. Also it allow to study the various aspects of very complex and huge applications like aero plane, rocket, submarine etc on computer without physically testing them in wind tunnel (which is impossible). Hence it save millions of rupees in design aspect and also increases the performance of the various fluid related appliances. In future, with more efficient and developed computer technology CFD will become the basic necessity of industries.

References

[1]. Craft T.J. et al. Int. J. Heat Mass Transfer. 1993. **36**. 2685–2697p.
[2]. Merci B. et al. Int. J. Numer. Methods Heat Fluid Flow. 2003. **13**. 110–132p.
[3]. Papageorgakis G.C. et al.Numer. Heat Transfer. 1999. 35. 1–22p.
[4]. Hosseinalipour S.M. et al.Numer. Heat Transfer Part A. 1995. 28. 647–666p.
[5]. Mujumdar A.S. et al. Appl. Therm. Eng. 2005. 25. 31–44p.
[6]. Gibson M.M. et al. Int. J. Heat Fluid Flow. 1997. 18. 80–87p.
[7]. Wilcox D.C. DCW Industries. 2002.